

Neutron imaging at the n_TOF facility of CERN

M. Bacak^{1,2,*}, F. Mingrone¹, M. Calviani¹, C. Torregrosa Martin¹, O. Aberle¹, E. Chiaveri^{1,3,4}, E. Fornasiere¹, A. Perillo-Marcone¹, V. Vlachoudis¹, and the n_TOF Collaboration¹

¹European Organization for Nuclear Research, CERN, CH-1211 Geneva, Switzerland

²Technische Universität Wien, 1040 Wien, Austria

³University of Manchester, M13 9PL Manchester, UK

⁴Universidad de Sevilla, 41004 Sevilla, Spain

Abstract. A neutron radiography station has been developed at the n_TOF facility of CERN. The characteristics of the neutron beam line and the imaging setup are presented in this paper together with first experimental results. A comparison of two different collimation systems is discussed and further improvements and upgrades are outlined.

1 Introduction

Neutron imaging is a non-destructive analysis method for a variety of applications [1–3]. Due to their properties, neutrons are excellent probes able to penetrate thick-walled samples. Images of the transmitted radiation, which intensity depends on the thickness of the material layers and on the specific attenuation properties of that material, can be created. In this regard neutrons can be compared to X-rays, but while X-rays are attenuated more effectively by materials with high-Z, neutrons allow to image especially light materials such as hydrogenous compounds making the methods complimentary. Many neutron imaging facilities are operating worldwide [3] and recently a neutron radiography testing station has been developed [4, 5], exploiting the neutron beam at n_TOF Experimental Area 2 (EAR2). The characteristics of the n_TOF neutron beam for the imaging setup together with first results obtained will be presented and possible further developments of the neutron imaging capabilities of the n_TOF facility will be outlined.

2 Experimental Setup

2.1 The n_TOF facility

The neutron Time-Of-Flight facility n_TOF of CERN is based on an idea by C. Rubbia [6] and provides the nuclear scientific community with a powerful tool for the measurement of neutron-induced cross-sections since 2001. In 2014 a vertical 20 m flight-path has been constructed complementing the existing horizontal 185 m one. At n_TOF neutrons are produced by spallation reactions induced by a 20 GeV/c pulsed proton beam from the CERN Proton Synchrotron on

a water-cooled lead target. The fast neutrons created in the spallation process are moderated in a 4 cm layer of demineralized light water towards experimental area 2 (EAR2), eventually covering 11 orders of magnitude from thermal energies up to several hundreds of MeV. Both beam lines are equipped with collimators to shape the neutron beam and a so-called sweeping magnet to deviate charged particles traveling along the neutron beam lines. Figure 1 shows the beam lines and their elements. Recently, the second experimental area (EAR2) [7] has been exploited as a neutron imaging facility [8]. The collimation system in EAR2 consists of a first collimator, a sweeping magnet, a so-called filter box and a second collimator. The second collimator defines the neutron beam parameters in the experimental area and is shown in Figure 2 together with a magnified image of the shape of the collimator. This shape was chosen to optimize neutron cross-section measurements, without taking

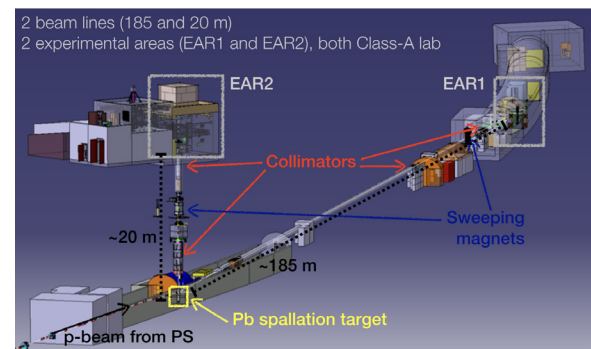


Figure 1: Scheme of the n_TOF facility. The main component of the neutron source and the two neutron beam-lines are highlighted.

*e-mail: michael.bacak@cern.ch

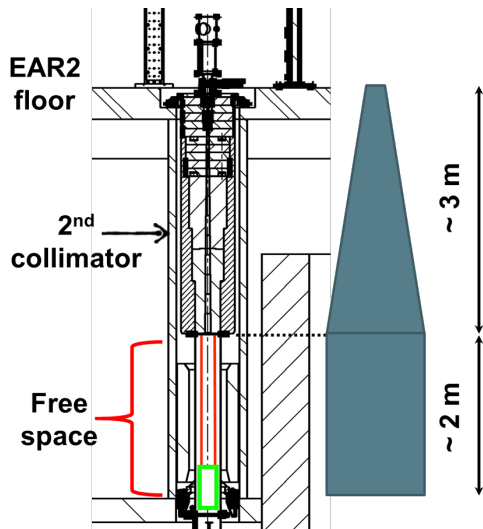


Figure 2: Scheme of the second collimator in EAR2. On the right side an magnified image of the second collimator is given to better illustrate its shape.

into account the requirements for the recent imaging applications, where a pinhole collimator would be preferred. Two versions of the second collimator, called small and big, are in use at n_TOF EAR2, with apertures of 70 mm and 96.5 mm. The resulting thermal ($E_n < 1\text{ eV}$) neutron flux is about $5 \cdot 10^5 - 8 \cdot 10^5 \text{ n/cm}^2/\text{pulse}$ for the small and the big collimator respectively. The distance between the collimator entrance aperture and the floor of EAR2 is approximately 3 m, as can be seen in Figure 2.

2.2 Imaging station

The samples are positioned on a remotely controlled sample holder, able to move the sample in the horizontal plane, in a height of 2 m from the floor of EAR2, thus 5 m from the aperture of the second collimator. The detection system consists of a commercially available sCMOS camera with an active input area of $13.3 \times 13.3 \text{ mm}^2$ mapped by $2048 \text{ pixels} \times 2048 \text{ pixels}$. The camera is coupled to a $\text{ZnS}/^6\text{LiF}$ neutron scintillator, emitting photons with a wavelength of 520 nm, with an active area of $100 \times 100 \text{ mm}^2$ and a thickness of approximately $100 \mu\text{m}$. The external trigger signal for the acquisition of the camera, namely the trigger of the proton pulse, permits an optimization of the signal to background ratio. A photo of the beam line and a more detailed image of the detection system and measuring station is shown in the top and bottom panel of Figure 3, respectively.

3 Experimental results

Various samples have been inspected at n_TOF EAR2 using neutron imaging [8], and the experimental results are summarized in the following using

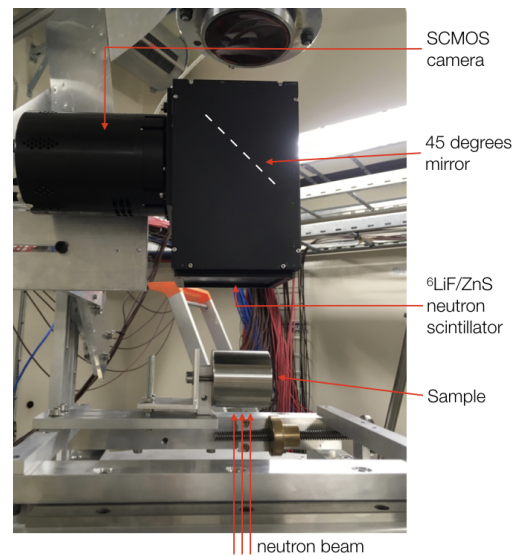
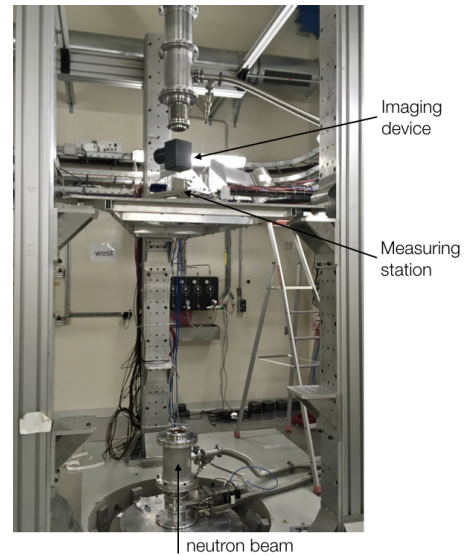


Figure 3: Beam line setup for the imaging measurements (left) and picture of the imaging setup (right), taken from [8].

a subset of the most significant measurements performed. In particular two samples related to R&D activities at CERN for the design of a new Antiproton Decelerator production Target (AD Target) [9] have been inspected:

- Non irradiated AD Target to proof the feasibility of neutron imaging at EAR2 and to investigate the differences in performance between the small and big collimator.
- One AD Target irradiated at the HiRadMat facility of CERN [10] to inspect the damage caused by the impact of proton beams on this target.

Both types of targets are similar in design and consist of an iridium core surrounded by a graphite matrix and a titanium alloy, as can be seen in Figure 4. In a first step the non irradiated AD target was inspected with the small and big collimator. The com-

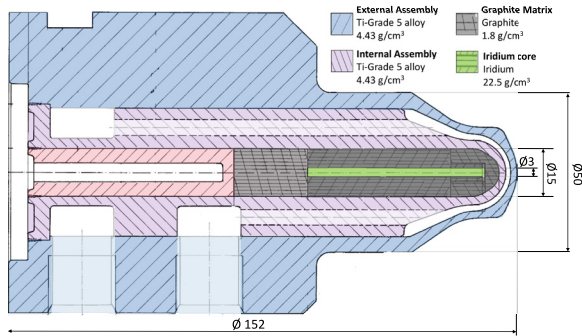


Figure 4: CAD drawing of the AD target, taken from [8].

parison of images of this dummy AD target are shown in the top and bottom panel of Figure 5 for the small and big collimator, respectively. In both cases the inner iridium core is clearly visible with good contrast, the feature that allowed to prove the feasibility of the technique. The small collimator offers a better spatial resolution due to the smaller aperture D , but at the same time has a smaller field of view, thus a smaller homogeneously irradiated area compared to the big collimator. In addition, the big collimator allows for a higher neutron intensity and therefore improved contrast. Following the successful proof of concept, a real target used in the Antiproton Decelerator (AD) of CERN have been inspected with the goal to identify potential material damage. Figure 6 shows the image of the irradiated AD target taken with the big collimator. If compared with the picture in the bottom panel of Figure 5 the iridium core does not show sharp edges anymore. With high probability those non-uniformities at the edges correspond to damage induced by the thermo-mechanical load of proton irradiation. A destructive mechanical inspection of the target is foreseen to confirm the hypothesis.

4 Future perspectives and improvements

The results shown in section 3 show the general feasibility of neutron imaging at n_TOF. However, improvements have to be done in order to achieve higher quality results. Mainly two components are responsible for the achieved quality of the images: the neutron beam line geometry and the detection system.

4.1 Beam line optics

The beam line influences three key quantities of the imaging facility and the achievable quality of the images:

- Contrast - given by the neutron fluence at the sample position.
- Spatial resolution - expressed as geometric blur $d = l/(L/D)$, where $l < L$ and L are the distances

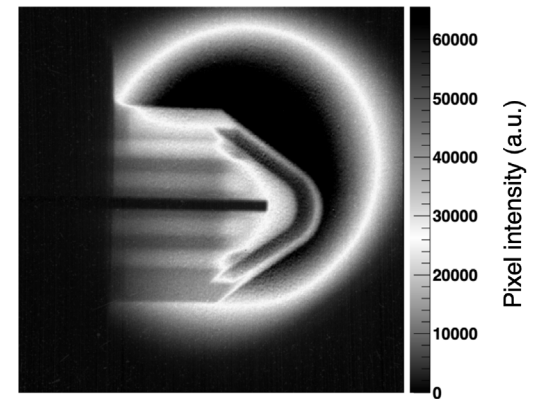
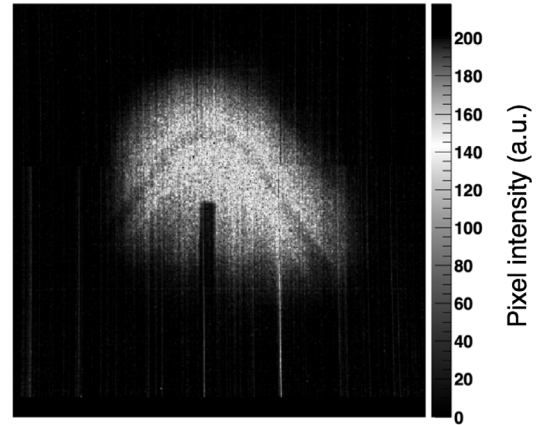


Figure 5: Comparison between the small (top) and big (bottom) collimator using a dummy AD target, taken from [8].

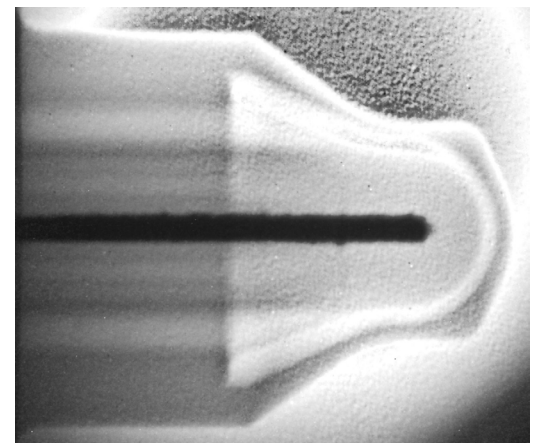


Figure 6: Image of the irradiated AD target. The inner iridium core (black) shows damage visible as non-uniformities at the edges, taken from [8].

between the sample position and an imaging device and between collimator aperture and sample position, respectively, and D is the aperture of the collimator.

- Field of view - the homogeneously irradiated area, intended as the full width at half maximum

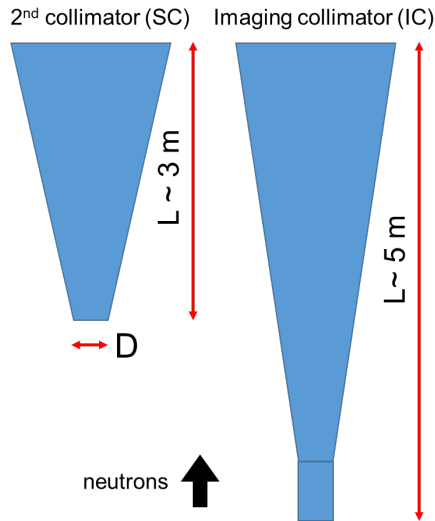


Figure 7: Potential new collimator designs for neutron radiography replacing the current small or big collimators at n_TOF EAR2. A pinhole camera design second collimator (left) and a new imaging collimator (right).

coll. system	D (mm)	Resolution L/D	FWHM (cm)	$\Phi_{th}/\Phi_{th}^{big}$ (%)
big	96.5	53.9	5.5	1
small	70	74.3	2.6	0.56
SC	100	52	11	0.91
IC	70	102.9	11.9	0.51

Table 1: Summary of the achievable resolution, field of view and contrast with respect to the big collimator for some selected collimation geometries.

(FWHM) of the neutron beam at sample position given by the aperture at the exit of the collimator.

At n_TOF the collimation system is more complex than a simple pinhole camera, and only the second collimator can be modified to optimize the optics, leaving the first untouched. Studies have been launched investigating new designs for a second collimator optimized for neutron imaging, as can be seen in Figure 7. The two designs are based on the available infrastructure at EAR2 and try to mimic the pinhole camera principle while considering radiation protection related matters. A new dedicated second collimator (SC) with opposite design with respect to the small and big collimators uses the same outer geometries as the existing collimators. A new dedicated imaging collimator (IC) allows to increase the distance between collimator aperture D and the sample by an additional 2 m, therefore improving the spatial resolution. It however does require more investigation with respect to the mechanical feasibility. Table 1 compares the quality criteria of the new collimator designs

with the existing ones for selected parameters of the aperture D . With the new designs a much larger field of view is achievable. The resolution is similar or better compared to the big collimator but the thermal neutron fluence Φ_{th} decreases.

4.2 Detection system

During the measurements it was observed that the ZnS scintillator was degrading over time, probably due to the fast neutrons in the n_TOF neutron beam. Apart from imaging with thermal neutrons, using the epithermal neutron flux by coupling the imaging system with a faster scintillator could allow to study the material compositions using Resonance Shape Analysis of the (n,γ) reaction. In addition, fast neutron detectors, for example Micro Channel Plates, could open the possibility of taking material selective radiographs gating on neutron resonances of given isotopes.

5 Summary

The feasibility of neutron radiography at n_TOF at CERN has been successfully proven. The performance of two collimation systems, not optimized for neutron imaging, has been compared and for a first experiment the setup has been chosen to maximize the contrast (i.e. the neutron fluence) and the field of view. For the future, a new dedicated collimation system is being designed to improve the field of view and the achievable resolution preserving the high neutron flux necessary for a good imaging contrast. An upgrade to the detection system is also foreseen, together with the use of specific masks in order to fully characterize the performance of the neutron imaging station at EAR2 in 2021.

References

- [1] J.S. Brenizer, Phys. Procedia **43**:10–20 (2013)
- [2] R. Woracek et al., Nucl. Instr. Meth. A **878**:141–158 (2018)
- [3] E.H. Lehmann, J. Imaging **3**(4), 52 (2017)
- [4] M. Calviani et al., CERN-INTC-2014-070. INTC-I-160, CERN (2014)
- [5] F. Mingrone, M. Calviani, CERN-INTC-2017-015. INTC-P-497, CERN (2017)
- [6] C. Rubbia et al., CERN/LHC/98-02, CERN (1998)
- [7] C. Weiss et al., Nucl. Instr. Meth. A **799**:90–98 (2015)
- [8] F. Mingrone et al., Instruments **3**(2), 32 (2019)
- [9] M. Torregrosa et al., Mater. Des. Process. Commun. **1**, e38 (2019)
- [10] I. Efthymiopoulos et al., In Proceedings of the IPAC2011, San Sebastian, Spain, 4–9 September, pp. 1665–1667 (2011)